K-ras and Wnt Signaling Synergize to Accelerate Prostate Tumorigenesis in the Mouse

Helen B. Pearson, Toby J. Phesse, and Alan R. Clarke

Cardiff University, School of Biosciences, Cardiff, Wales, United Kingdom

Abstract

Aberrant Ras and Wnt signaling are emerging as key events in the multistep nature of prostate tumorigenesis and progression. Here, we report the generation of a compound model of prostate cancer to define the synergism of activated K-ras (K-*ras*$^{+/V12}$) and dominant stabilized β-catenin (*Catnb*$^{+/lox(ex3)}$) in the murine prostate. Recombination of floxed alleles and subsequent expression of oncogenic transgenes was mediated by Cre recombinase expression governed by the composite Probasin (*PB*) promoter (termed *PBCre*). Concomitant with elevated mitogen-activated protein kinase (MAPK) signaling, *PBCre*$^{+}$*K-ras*$^{+/V12}$ mice developed AH at 100 days (100% incidence) and low-grade prostate intraepithelial neoplasia and adenocarcinoma (60% and 7% incidence) by 500 days. *PBCre*$^{+}$*Catnb*$^{+/lox(ex3)}$ mice showed reduced longevity (average 428 days) and were predisposed to PIN-like keratinized squamous metaplasia at 100 days (100% incidence) and adenocarcinoma (100% incidence) at end-point. These lesions displayed elevated Wnt signaling and basal levels of MAPK signaling. Synchronous activation of K-ras and β-catenin significantly reduced survival (average 189 days), reflecting accelerated tumorigenesis and the development of invasive carcinoma that displayed activated Wnt and MAPK signaling. Notably, expression of the basal cell marker p63 negatively correlated with tumor grade, resembling human prostate adenocarcinoma. Taken together, our data show that combinatorial oncogenic mutations of *K-ras* and *β-catenin* drive rapid progression of prostate tumorigenesis to invasive carcinoma, characterized by the synergistic elevation of androgen receptor, cyclooxygenase-2, and c-Myc. [Cancer Res 2009;69(1):94–101]

Introduction

Cancer development is a multistep process through which cells accumulate genetic mutations (1). Synchronous activation of Ras and Wnt signaling has been identified in several transgenic mouse tumor models, including the colon (2), intestine (3), kidney (3), breast (4), and liver (5). Homeostasis of the intestine is not affected in mice expressing a monoallelic K-*ras* activating mutation but can promote tumorigenesis in *Apc*-deficient mice (3). The convergence of the K-ras and Wnt signaling cascades to up-regulate the expression of genes that promote tumorigenesis, such as cyclooxygenase-2 (COX-2; ref. 6) and c-Myc (7, 8), indicates a direct synergy between these two pathways.

Between 17% and 25% of all human cancers are said to harbor an activating K-*Ras* mutation (9), with colonic (50%; ref. 2), pancreatic (90%; ref. 10), and lung (25–50%; ref. 11) malignancies exhibiting a high prevalence. However, H-*Ras* activating mutations are less abundant (<1%; ref. 9). In prostate cancer, Ras mutations are relatively uncommon (12). However, tissue microarray studies revealed Ras effector pathways to be up-regulated in prostate cancer, such as the mitogen-activated protein kinase (MAPK) and PI3K/AKT cascades (13, 14). Indeed, elevated p-ERK and p-AKT expression have been shown to correlate with tumor grade (13, 14). Up-regulation of Ras-mediated signaling cascades in the absence of oncogenic Ras mutations is considered to reflect the overexpression of autocrine and paracrine factors such as epidermal growth factor and transforming growth factor α, common to human prostate cancer (15).

Ras effector pathways are emerging as prime potential therapeutic targets for treating androgen-independent prostate cancer. The MAPK pathway has been shown to regulate an androgen receptor (AR)-sensitive reporter in human prostate cancer cell lines (16), whereas p-ERK has been shown to mediate androgen signaling by phosphorylating AR coactivators, including the steroid receptor coactivator and ARA70 (16).

To date, *in vivo* prostate cancer models expressing activating mutations in *Ras* have generated a variety of low-grade prostate phenotypes, considered to reflect differences in the transgenes and the genetic background used (17). Transgenic mice expressing activated H-Ras from the human T24 human bladder carcinoma cell line (*Ha-RasT24*^{G12V}) under control of the *PB* promoter developed atypical hyperplasia (AH) in the dorsolateral and ventral lobes of the prostate between ages 6 to 12 months (18). More recently, Scherl and colleagues (17) showed that mice expressing a G12V point mutation in cH-Ras (termed *H-Ras*^{V12}), under the control of the minimal *PB* promoter, developed low-grade prostate intraepithelial neoplasia (LG-PIN) that displayed intestinal metaplasia by 3 months. At 12 months, the *H-Ras*^{V12} transgene was not detected in this model, coinciding with a decrease in PIN incidence. This suggests that Ras signaling was necessary to maintain the phenotype. Together, these models show that activated Ras can facilitate prostate tumorigenesis and early stage tumor development.

Studies using mouse prostate reconstitution (MPR) models have provided evidence that further mutations/genetic events are required for the development of advanced prostate lesions in the context of an activating *Ras* mutation. Introduction of activated *vHa-Ras*^{V12} or *c-Myc* into the fetal urogenital sinus (UGS) by recombinant retroviral vectors caused dysplasia and hyperplasia, respectively, when transplanted into the renal capsule of an adult isogenic male host (19). However, in combination, activated Ras and c-Myc cooperate to facilitate progression to carcinoma (19). The multistep nature of tumorigenesis was further shown in the MPR model, where loss of p53 and activation of Ras and c-Myc induced prostate carcinoma that metastasised to the lung, liver, small intestine, bone, and mesentery (20).

Note: Supplementary data for this article are available at Cancer Research Online (http://cancerres.aacrjournals.org/).

Requests for reprints: Alan R. Clarke, Cardiff University, School of Biosciences, Museum Avenue, Cardiff, CF10 3US, Wales, United Kingdom. Phone: 44-0-2920-879115; Fax: 44-02920-874116; E-mail: clarkear@cardifff.ac.uk.

doi:10.1158/0008-5472.CAN-08-2895

Activating mutations and overexpression of β-catenin have been detected in a variety of human malignancies including colorectal, hepatocellular, ovarian, and prostate cancer (21). The β-catenin (CTNNB1) oncogene is a critical regulator of the Wnt pathway, essential for normal mammalian development, polarity, and migration, as well as forming adherens junctions at the cell surface membrane (22). Recently, a growing body of evidence has implicated aberrant Wnt signaling and its convergence with the androgen signaling pathway as critical events in (human or mouse) prostate tumorigenesis (23, 24).

The role of deregulated Wnt signaling in prostate tumorigenesis has been shown in several conditional transgenic mouse prostate models. Mouse mammary tumor virus (MMTV)-Cre mediated dominant stabilization of β-catenin in the prostate been shown to predispose to PIN-like keratinized squamous metaplasia (25, 26), whereas deletion of the β-catenin regulator APC, mediated by *PBCre*, results in androgen-independent prostate adenocarcinoma (27), highlighting the importance of the Wnt cascade during tumorigenesis and disease progression.

To determine whether the Wnt and K-ras pathways synergize during prostatic tumorigenesis, the Cre-loxP system was used to conditionally activate K-ras ($K\text{-}ras^{+/V12}$) and/or dominant stabilized β-catenin ($Catnb^{+/\Delta ex3}$) in the prostate. We show for the first time that K-ras activation causes a prostate phenotype (AH and LG-PIN), resembling activated $H\text{-}ras^{V12}$ prostate cancer models (17–19). $PBCre^{+}Catnb^{+/\Delta ex3}$ mice displayed high-grade PIN-like keratinized squamous metaplasia and adenocarcinoma that were phenotypically distinct to $PBCre^{+}K\text{-}ras^{+/V12}$ prostate lesions. In double mutants, disease progression was accelerated to invasive carcinoma that displayed elevated COX-2, c-Myc, and AR, which are regulated by both the Ras and Wnt pathways. Together, these data support the concept that Ras and Wnt signaling cooperate to promote prostate tumorigenesis.

Materials and Methods

Experimental animals. All animal studies and breeding were carried out under UK Home Office regulations. The *PB-Cre4* (ARR_2PB) mice were obtained from the Mouse Models of Human Cancers Consortium (National Cancer Institute-Frederick). $K\text{-}ras^{LSLV12}$ and $Catnb^{+/lox(ex3)}$ mice have been described previously (28, 29). Mice were backcrossed six times onto a C57 Bl/6 background. The *PBCre* transgene was incorporated into cohorts using male mice, as $PBCre^{+}$ female mice have been shown to recombine in the ovaries (30). Cohorts were aged to 500 d or sacrificed upon signs of failing health.

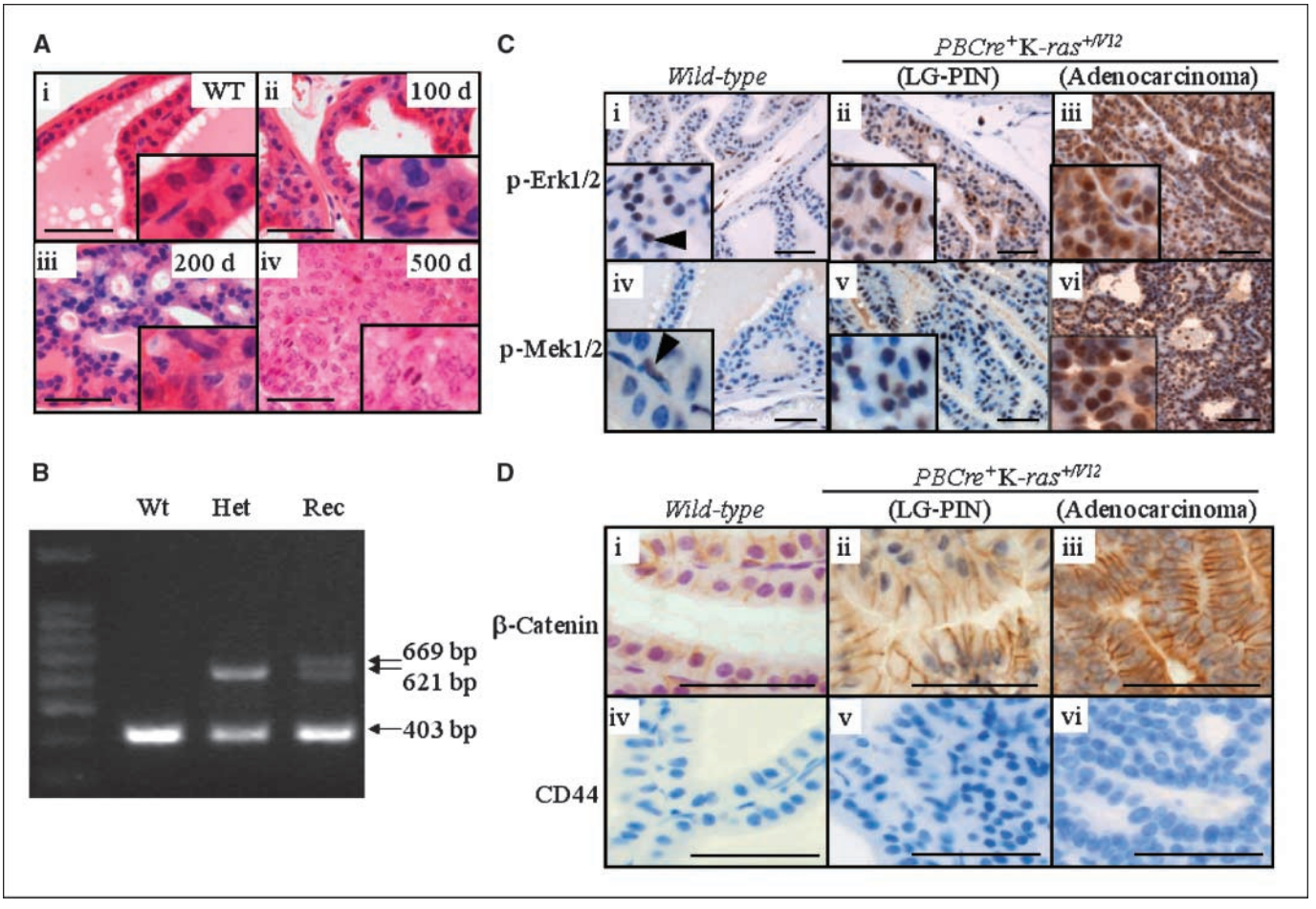

Figure 1. $PBCre^{+}K\text{-}ras^{+/V12}$ prostate lesions display elevated Ras signaling. *A,* H&E stained prostate sections of (*i*) *wild-type* (500 d) and $PBCre^{+}K\text{-}ras^{+/V12}$ focal AH at 100 d (*ii*), LG-PIN at 200 d (*iii*), and diffuse adenocarcinoma at 500 d (*iv*). *Inserts,* nuclear atypia (*ii* and *iii*) and mitotic bodies (*iv*). *B,* PCR analysis revealed that $PBCre^{+}K\text{-}ras^{+/V12}$ prostate lesions (*Rec*) expressed the recombined $K\text{-}ras^{V12}$ allele (621 bp), whereas *wild-type* (*Wt*; 403 bp) and $PBCre^{+}K\text{-}ras^{+/V12}$ (*Het*; 669 bp) tail DNA served as controls ($n = 3$). *C,* IHC to detect p-Erk1/2 (*i–iii*) and p-Mek1/2 (*iv–vi*) in *wild-type* and $PBCre^{+}K\text{-}ras^{+/V12}$ prostate indicates elevated MAPK signaling in the lesions. *D,* IHC to detect β-catenin (*i–iii*) and CD44 (*iv–vi*) in *wild-type* and $PBCre^{+}K\text{-}ras^{+/V12}$ prostate indicates no Wnt deregulation in the lesions. Images were taken from the anterior lobe at ×40 magnification; *scale bars,* 50 μm.

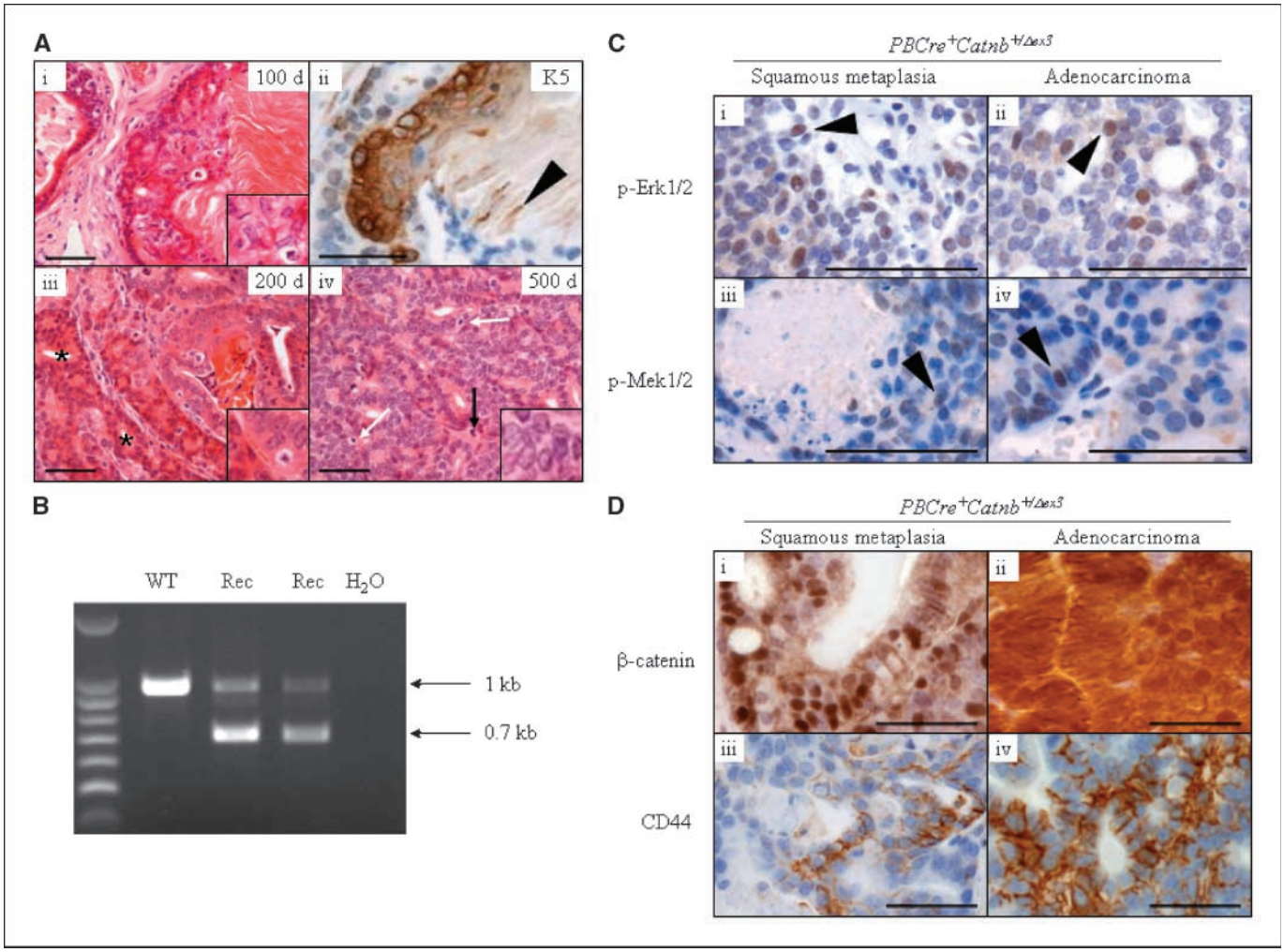

Figure 2. *PBCre*$^{+}$Catnb$^{+/lox(ex3)}$ mice develop prostate lesions that display elevated Wnt signaling. *A,* H&E analysis to show *PBCre*$^{+}$*Catnb*$^{+/\Delta ex3}$ mice develop high-grade PIN-like lesions that manifested keratinized squamous metaplasia lesions at 100 d (*i*), which displayed apoptotic bodies (*insert*). Keratin whorls and keratinocytes (*arrowhead*) stained positively for cytokeratin-5 (*ii*). At 200 d, PIN-like keratinized squamous metaplasia and adenocarcinoma were present, which displayed rosette structures (*; *iii*). End point *PBCre*$^{+}$*Catnb*$^{+/\Delta ex3}$ mice manifested diffuse and locally invasive adenocarcinomas associated with mitosis (*black arrow*) and apoptosis (*white arrow*). *B,* PCR analysis revealed that *wild-type* prostate (*lane 1*) was not recombined (~1 kb product), whereas *PBCre*$^{+}$*Catnb*$^{+/\Delta ex3}$ lesions at 100 d (*lane 2*) and 500 d (*lane 3*) were recombined (0.7 kb product; $n = 3$). *C,* IHC to detect p-ERK (*i–ii*) and p-MEK (*iii–iv*) in *wild-type* and *PBCre*$^{+}$*Catnb*$^{+/\Delta ex3}$ lesions at 100 d (*squamous metaplasia*) and 500 d (*adenocarcinoma*). *D,* IHC revealed that *PBCre*$^{+}$*Catnb*$^{+/\Delta ex3}$ lesions display elevated nuclear β-catenin (*i–ii*) and CD44 at the cell surface (*iii–iv*). All images were taken at ×40 magnification; *scale bars,* 50 μm.

Genotyping. Mice were genotyped from DNA isolated from tail biopsies as described previously for K-*ras*^{LSLV12} floxed/recombined alleles (28) and *Cre Recombinase* (31). Floxed β-*catenin* alleles were detected using Catnb-F 5′-CTGCGTGGACAATGGCTACT-3′ and Catnb-R 5′-TCCATCAGGT-CAGCTGTAAAAA-3′ (324 bp and 500 bp products produced for wild-type and floxed alleles, respectively). Detection of the dominant stabilized *β-catenin*–recombined allele has been described previously (29).

Tissue isolation and histology. Histologic analysis of the genitourinary (GU) tract was done in accordance with the consensus report from the Bar Harbor meeting of the mouse models of human cancer consortium prostate pathology committee (32). Tissue was harvested as described previously (33) and fixed for no longer than 24 h in 10% neutral buffered formaldehyde at 4°C, embedded in paraffin, and sectioned at 5 μm. Sections were stained with H&E for histologic analysis.

Immunohistochemistry. Immunohistochemistry (IHC) was carried out as described previously (33). Primary antibodies were obtained from the following sources: AR (#RB-1358-P0; Lab Vision Corporation), β-catenin (#C19220; BD Transduction Laboratories), CD44 (#550538; Pharmingen), Keratin-5 (#PRB-160P; Covance), Ki-67 (#VP-K452; Vector Laboratories), p63 (#MS-1081; LabVision), p-Erk1/2 (Thr 202/Tyr204; #4376, Cell Signaling Technology), p-Mek1/2 (Ser221; #2338; Cell Signaling Technology), COX-2 (#RP-9072-P0; LabVision), and c-Myc (Santa Cruz #SC-764).

Scoring. The percentage of basal (p63 positive), proliferating (Ki-67 positive), AR, COX-2, and c-Myc–positive cells was determined by counting the total positive and negative cells from 20 acini, or in the case of prostate lesions, from 20 random 2,500 μm^2 regions using "AnalySIS" software (Olympus Soft Imaging System; GMBH) at ×40 magnification (a minimum of 1,000 cells per mouse were counted), where $n = 3$. Statistical analysis was carried out using the nonparametric Mann-Whitney Test (95% confidence interval).

Results

***PBCre*$^{+}$K-*ras*$^{+/V12}$ mice develop prostate cancer.** To investigate the role of activated Ras signaling within the prostate, we crossed the *PBCre* transgenic line to mice harboring a conditional oncogenic K-*ras*^{V12} allele (28). Male cohorts of *wild-type* (*PBCre*$^{+}$ K-*ras*$^{+/+}$) and mutant (*PBCre*$^{+}$K-*ras*$^{+/V12}$) mice were generated and observed for signs of illness. To monitor disease progression we examined cohorts at 100 ($n = 6$), 200 ($n = 6$), and 500 ($n \geq 17$) days.

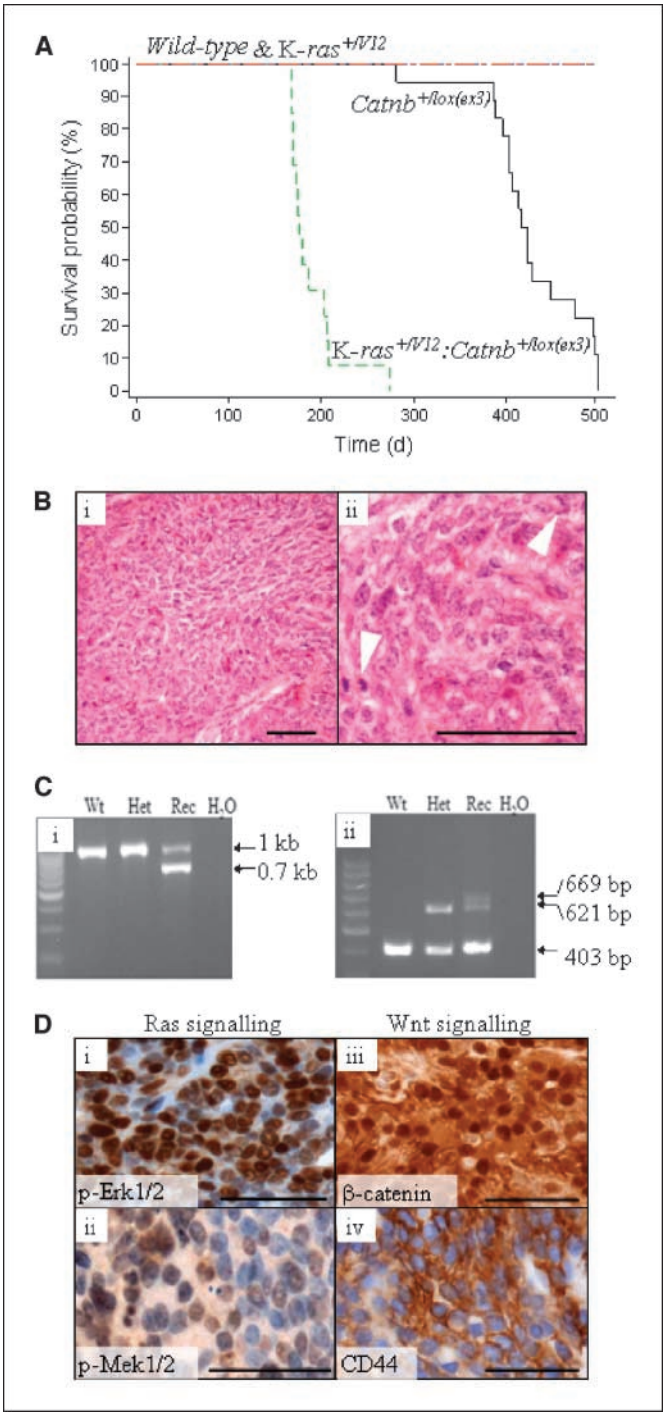

Figure 3. Combined activation of β-catenin and K-ras reduces male longevity and accelerated prostate tumor progression. *A,* Kaplan-Meier survival curve. *PBCre*$^{+}$*Catnb*$^{+/lox(ex3)}$:K-*ras*$^{+/V12}$ longevity (*green*; average survival, 189 d) is significantly reduced compared with *wild-type* (*red*; average survival, 500 d), K-*ras*$^{+/V12}$ (*blue*; average survival, 500 d) and *Catnb*$^{+/lox(ex3)}$ (*black*; average survival, 428 d) cohorts (χ^2 = 48.66, P = 0.000; χ^2 = 48.66, P = 0.000; and χ^2 = 31.89, P = 0.000, respectively). *B,* H&E analysis of *PBCre*$^{+}$*Catnb*$^{+/\Delta ex3}$:K-*ras*$^{+/V12}$ invasive prostate carcinoma at low (*i*) and high (*ii*) magnification, showing loss of glandular architecture, mitotic bodies (*arrowheads*), and nuclear atypia. *C,* PCR analysis of *wild-type* and *PBCre*$^{+}$*Catnb*$^{+/lox(ex3)}$:K-*ras*$^{+/V12}$ tail biopsies and prostate lesions confirmed that invasive carcinoma lesions express recombined *β-catenin* (*i*) and K-*ras* (*ii*) alleles (n = 3). *D,* IHC to detect p-ERK (*i*), p-MEK (*ii*), β-catenin (*iii*), and CD44 (*iv*) in *PBCre*$^{+}$*Catnb*$^{+/\Delta ex3}$:K-*ras*$^{+/V12}$ invasive carcinomas, revealing elevated Ras/MAPK and Wnt signaling. Images were taken at ×40 magnification; *scale bars,* 50 μm.

No gross phenotype was observed in *wild-type* mice (n = 32), whereas the *PBCre*$^{+}$K-*ras*$^{+/V12}$ cohort (n = 17) was predisposed to prostate lesions in all 4 lobes of the prostate (Fig. 1*A*). At 100 days, *PBCre*$^{+}$K-*ras*$^{+/V12}$ mice displayed infrequent AH. AH composed of focal tufting with nuclear abnormalities, including enlargement and the increased prominence of nucleoli. At 200 days, *PBCre*$^{+}$K-*ras*$^{+/V12}$ mice displayed localized AH and progression to LG-PIN with 100% and 67% incidence, respectively. LG-PIN foci displayed small solid and cribriform intraluminal proliferation of markedly atypical epithelial cells, which was accompanied by nuclear atypia (32). Aged *PBCre*$^{+}$K-*ras*$^{+/V12}$ mice all survived to the 500 day end point and displayed frequent focal AH (93% incidence), LG-PIN (60% incidence), and in 1 case, diffuse adenocarcinoma.

Excision of the transcriptional STOP cassette within the K-*ras*$^{+/V12}$ transgene (28) was confirmed within the *PBCre*$^{+}$K-*ras*$^{+/V12}$ prostate lesions (at 500 days) by PCR from tumor DNA (Fig. 1*B*). *Wild-type* and *PBCre*$^{+}$K-*ras*$^{+/V12}$ tail DNA served as negative controls.

***PBCre*$^{+}$K-*ras*$^{+/V12}$ prostate lesions display aberrant Ras signaling.** To validate the hyperactivation of K-*ras*, we used IHC to monitor the expression of MAPK signaling components. Nuclear and cytoplasmic levels of activated p-Erk1/2 (Thr202/Tyr204) and p-Mek1/2 (Ser 221) were significantly elevated in K-*ras*$^{+/V12}$ prostate lesions compared with controls (Fig. 1*C*), positively correlating with severity. These data indicate that stimulation of the MAPK pathway might be required for tumor progression.

To determine whether aberrant Ras signaling deregulated the Wnt pathway, we analyzed the expression of β-catenin (Fig. 1*D*). Although β-catenin was predominantly expressed on the cell surface in control prostate epithelium and *PBCre*$^{+}$K-*ras*$^{+/V12}$ mutants, nuclear β-catenin was rarely detected (Fig. 1*D*). These data strongly suggest that elevated Ras signaling in prostate epithelium does not deregulate canonical Wnt signaling. In accordance with this, the Wnt/β-catenin target CD44 is also not up-regulated in *PBCre*$^{+}$K-*ras*$^{+/V12}$ prostate lesions.

***PBCre*$^{+}$*Catnb*$^{+/lox(ex3)}$ mice develop PIN-like keratinized squamous metaplasia and prostate adenocarcinoma.** To investigate the role of Wnt signaling in prostate tumorigenesis, *PBCre*$^{+}$ transgenic mice were intercrossed with mice heterozygous for the dominant stabilized form of β-catenin (*Catnb*$^{+/lox(ex3)}$). Male cohorts of *wild-type* and *PBCre*$^{+}$*Catnb*$^{+/lox(ex3)}$ mice were examined at 100 (n = 6) and 200 (n = 6) days to monitor disease progression and at 500 days or when they became sick ($n \geq 18$). The average survival of the *PBCre*$^{+}$*Catnb*$^{+/lox(ex3)}$ cohort (n = 18) was significantly reduced to 428 days (χ^2 = 34.56, P = 0.000; Fig. 3*A*).

Histologic analysis revealed that although *wild-type* prostate developed normal, ordered epithelium, *PBCre*$^{+}$*Catnb*$^{+/lox(ex3)}$ mice developed lesions in all four prostate lobes (Fig. 2*A*). At 100 days, *PBCre*$^{+}$*Catnb*$^{+/lox(ex3)}$ mice (n = 6) manifested diffuse high grade PIN-like keratinized squamous metaplasia (Fig. 2*Ai*). These lesions displayed nuclear atypia, apoptotic bodies, mitotic figures, and extensive overcrowding of the lumen as multicellular disorganized layers form. IHC to detect cytokeratin-5 expression (a prostate basal cell marker) confirmed the development of keratinization within multiple foci of squamous metaplasia (Fig. 2*Aii*). At 200 days, *PBCre*$^{+}$*Catnb*$^{+/lox(ex3)}$ mice developed high-grade PIN-like keratinized squamous metaplasia and adenocarcinoma foci (Fig. 2*Aiii*). Adenocarcinoma lesions displayed nuclear atypia and cells formed rosette-like structures indicating glandular differentiation is maintained (32). At end-point, hyperactivation of β-catenin led to diffuse and locally invasive adenocarcinomas with 100% incidence in *PBCre*$^{+}$*Catnb*$^{+/lox(ex3)}$ mice (Fig. 2*Aiv*). Adenocarcinomas showed

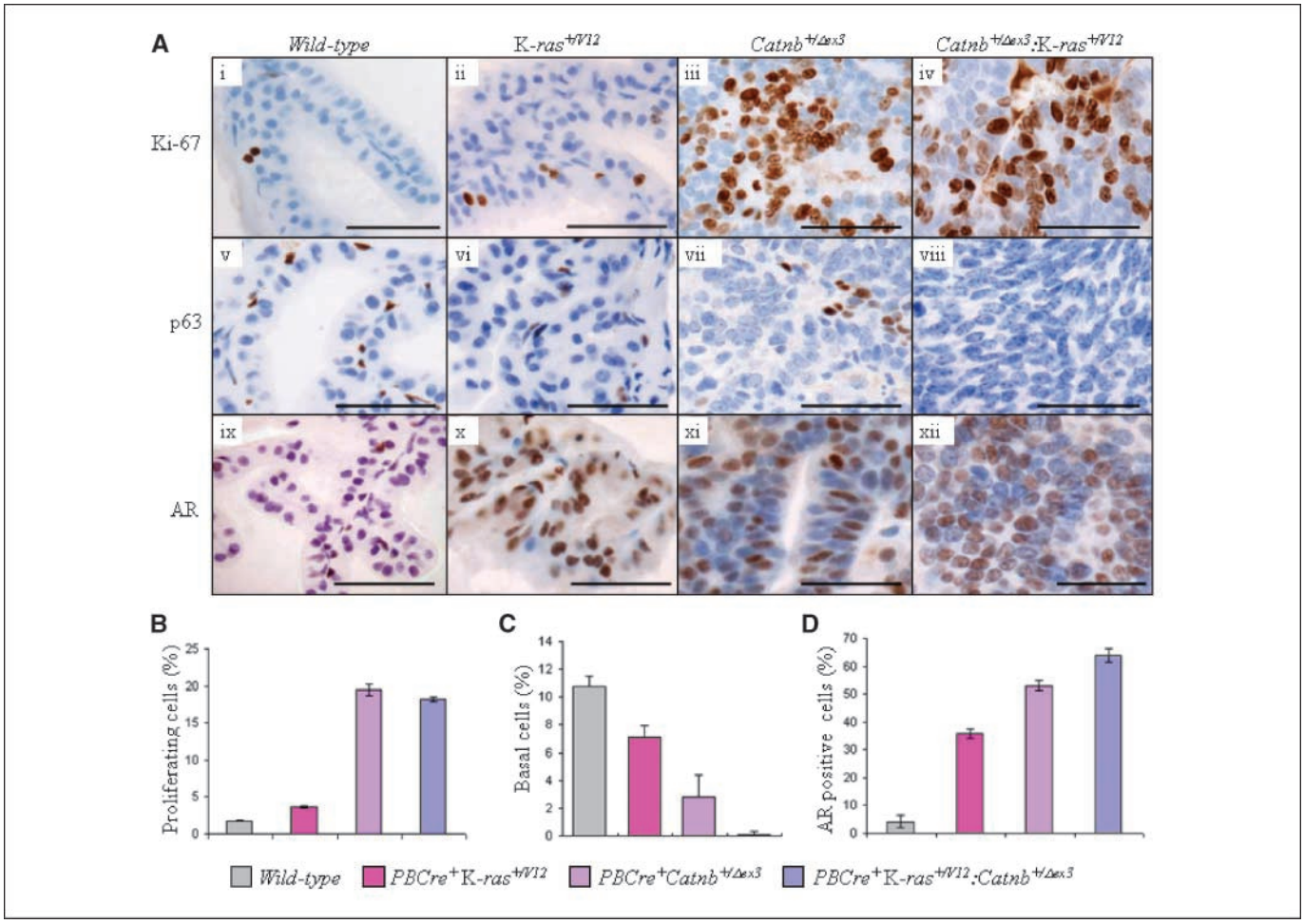

Figure 4. Characterization of activated β-catenin and K-ras synergy in prostate lesions. *A,* IHC to detect Ki-67 (*i–iv*), p63 (*v–viii*), and AR (*ix–xii*) expression in *PBCre*$^{+}$*K-ras*$^{+/V12}$, *PBCre*$^{+}$*Catnb*$^{+/\Delta ex3}$, and *PBCre*$^{+}$*Catnb*$^{+/\Delta ex3}$*:K-ras*$^{+/V12}$ prostate tumors at end time points. Images were taken at ×40 magnification; *scale bars,* 50 μm. The percentage of Ki-67 (*B*), p63 (*C*), and AR-positive (*D*) prostate epithelial cells were scored for each genotype (n = 3), revealing that *PBCre*$^{+}$*K-ras*$^{+/V12}$, *PBCre*$^{+}$*Catnb*$^{+/\Delta ex3}$, and *PBCre*$^{+}$*Catnb*$^{+/\Delta ex3}$*:K-ras*$^{+/V12}$ prostate tumors showed a significant difference in Ki-67, p63, and AR expression compared with *wild-type* mice (P = 0.0404) and to each other (P = 0.0404). *Columns,* mean; *bars,* SD; statistical analysis was carried out using a nonparametric Mann-Whitney test (95% confidence interval).

increased severity compared with those at 200 days and keratinized squamous metaplasia was rarely detected. Notably, these lesions resembled the *MMTV-Cre*$^{+}$*Catnb*$^{+/lox(ex3)}$ and *PBCre*$^{+}$*Apc*$^{fl/fl}$ models described previously (25–27). Indeed, prostate cancer progression in *PBCre*$^{+}$*Catnb*$^{+/lox(ex3)}$ mice closely mirrors that of *Apc* mutant mice, consistent with Wnt signaling deregulation.

Monoallelic deletion of exon 3 (amino acids 5–80) and subsequent stabilization of β-catenin was confirmed in both PIN-like keratinized squamous metaplasia and adenocarcinoma lesions by PCR analysis of tumor DNA (Fig. 2*B*).

***PBCre*$^{+}$*Catnb*$^{+/lox(ex3)}$ mice display elevated Wnt signaling.** To determine whether dominant stabilization of β-catenin drives tumorigenesis by stimulating the Ras and Wnt signaling pathways, IHC was carried out to detect the activated MAPK signaling molecules p-Erk1/2 and p-Mek1/2 (Fig. 2*C*) and the Wnt signaling component β-catenin and its transcriptional target CD44 (Fig. 2*D*). *PBCre*$^{+}$*Catnb*$^{+/\Delta ex3}$ prostate lesions displayed elevated β-catenin expression in the nucleus, concomitant with up-regulated CD44 expression, strongly suggestive of activated Wnt signaling (34). The MAPK cascade is not deregulated in *PBCre*$^{+}$*Catnb*$^{+/\Delta ex3}$ prostate lesions, as p-Erk1/2 and p-Mek1/2 expression was not markedly increased compared with *wild-type* prostate epithelium (shown previously in Fig. 1*C*). This strongly suggests that endogenous K-*ras* is not active in these mice and that K-*ras* hyperactivation alone (at 500 days) is unable to progress tumorigenesis to the squamous metaplasia observed in the *PBCre*$^{+}$Catnb$^{+/\Delta ex3}$ mice.

***PBCre*$^{+}$*Catnb*$^{+/lox(ex3)}$ male mice develop multiple GU tract squamous metaplasias.** In addition to prostate lesions, the *PBCre*$^{+}$*Catnb*$^{+/lox(ex3)}$ cohort was also predisposed to a number of additional GU tract phenotypes. Bulbourethral gland keratinized squamous metaplasia was observed with 100% incidence at all time points analyzed (Supplementary Fig. S1*A*). Keratinized squamous metaplasia of the preputial gland was observed at 100 days (67% incidence), 200 days and at end-point (100% incidence; Supplementary Fig. S1*B*), which is consistent with the *MMTV-Cre*$^{+}$*-Catnb*$^{+/lox(ex3)}$ model (26). In addition, urethral keratinized squamous metaplasia was observed at 200 days and at end-point (17% and 28% incidence, respectively; Supplementary Fig. S1*C*).

***PBCre*$^{+}$*Catnb*$^{+/lox(ex3)}$*:K-ras*$^{+/V12}$ mice show reduced longevity.** To investigate the potential cooperative role between Ras and Wnt signaling in prostate tumorigenesis, we generated a cohort of male mice heterozygous for both activated K-*ras*^{V12} and the dominant

stable form of *β-catenin*, using the *PBCre* transgene to mediate expression (n = 13). Double mutants displayed a significant reduction in longevity (average survival, 189 days) compared with other cohorts (χ^2 = 48.66; P = 0.000; Fig. 3*A*), indicating that K-ras and β-catenin synergize to accelerate tumorigenesis in the prostate.

***PBCre*$^+$*Catnb*$^{+/lox(ex3)}$*:K-ras*$^{+/V12}$ mice develop invasive prostate carcinoma.** Histologic analysis revealed that *PBCre*$^+$*Catnb*$^{+/lox(ex3)}$*:K-ras*$^{+/V12}$ mice were predisposed to diffuse, locally invasive carcinoma (100% incidence) that developed from solid or sheet-like proliferations with occasional rosette structures, nuclear atypia, apoptotic bodies, and mitosis (Fig. 3*B*). PCR analysis confirmed that recombination of the LoxP-flanked K-*ras*^{V12} and β-*catenin* alleles had taken place in *PBCre*$^+$*Catnb*$^{+/\Delta ex3}$*:K-ras*$^{+/V12}$ prostate lesions (Fig. 3*C*).

In addition to prostate carcinoma, the double mutant cohort also developed bulbourethral, preputial, and urethral gland keratinized squamous metaplasias, mirroring *PBCre*$^+$*Catnb*$^{+/lox(ex3)}$ mice. Synchronous activation of Ras and Wnt signaling was also detected in the testis, predisposing to male infertility (83% incidence). Double mutants displayed hypospermatogenesis and AH of the epididymis and ductus deferens, which corresponded to *PBCre*-mediated recombination, determined by the surrogate Rosa26 allele (Supplementary Fig. S2).

***PBCre*$^+$*Catnb*$^{+/lox(ex3)}$*:K-ras*$^{+/V12}$ invasive carcinoma displays synergy between activated Ras and Wnt signaling.** IHC revealed that *PBCre*$^+$*Catnb*$^{+/\Delta ex3}$*:K-ras*$^{+/V12}$ invasive carcinomas displayed nuclear β-catenin and subsequent elevated CD44 expression, in addition to activated MAPK signaling proteins p-Erk1/2 and p-Mek1/2 (Fig. 3*D*). This differs from the single mutants, where only one signaling pathway was active and provides a clear rationale for the observed synergy.

Activated K-ras and β-catenin cause phenotypes similar to human prostate cancer. To characterize the synergistic relationship between dominant stabilization of β-catenin and activation of K-ras, we monitored the expression of the proliferation marker Ki-67, the basal cell marker p63 and AR by IHC (Fig. 4*A*), and scored the percentage of positive cells (Fig. 4*B–D*). *Wild-type* prostate showed a basal level of Ki-67–positive cells in the adult gland at 500 days (1.8%), which was increased in *PBCre*$^+$*K-ras*$^{+/V12}$ LG-PIN (3.7%) and more so in *PBCre*$^+$*Catnb*$^{+/\Delta ex3}$ adenocarcinomas (19.5%) and *PBCre*$^+$*Catnb*$^{+/\Delta ex3}$*:K-ras*$^{+/V12}$ invasive carcinomas (18.3%; P = 0.0404, Mann-Whitney; Fig. 4*B*). Slightly reduced Ki-67 staining in *PBCre*$^+$*Catnb*$^{+/\Delta ex3}$*:K-ras*$^{+/V12}$ lesions, compared with *PBCre*$^+$*Catnb*$^{+/\Delta ex3}$ mice (P = 0.0404, Mann-Whitney), probably reflects the increased incidence of necrotic cells associated with invasive carcinomas.

Notably, prostate lesions from all cohorts analyzed at end point showed clusters of enlarged, circular p63-positive cells, compared with the typical small, triangular-shaped basal cells of normal prostate epithelium (Fig. 4*Av–viii*). *Wild-type* prostate epithelial cells were 10.8% p63 positive (Fig. 4*C*), corresponding to previous work (35). Analysis of *K-ras* (LG-PIN), *β-catenin* (adenocarcinoma), and double transgenic (invasive carcinoma) mice at end point revealed that p63 expression decreases with prostate tumor progression (7.1%, 2.9%, and 0.1%, respectively). These data mimic human prostate cancer (27), bladder tumors (36), and head and neck squamous carcinoma (37).

IHC to detect AR revealed that as tumor stage progresses, nuclear AR accumulates in the neoplastic cells (Fig. 4*Aix–xii*).

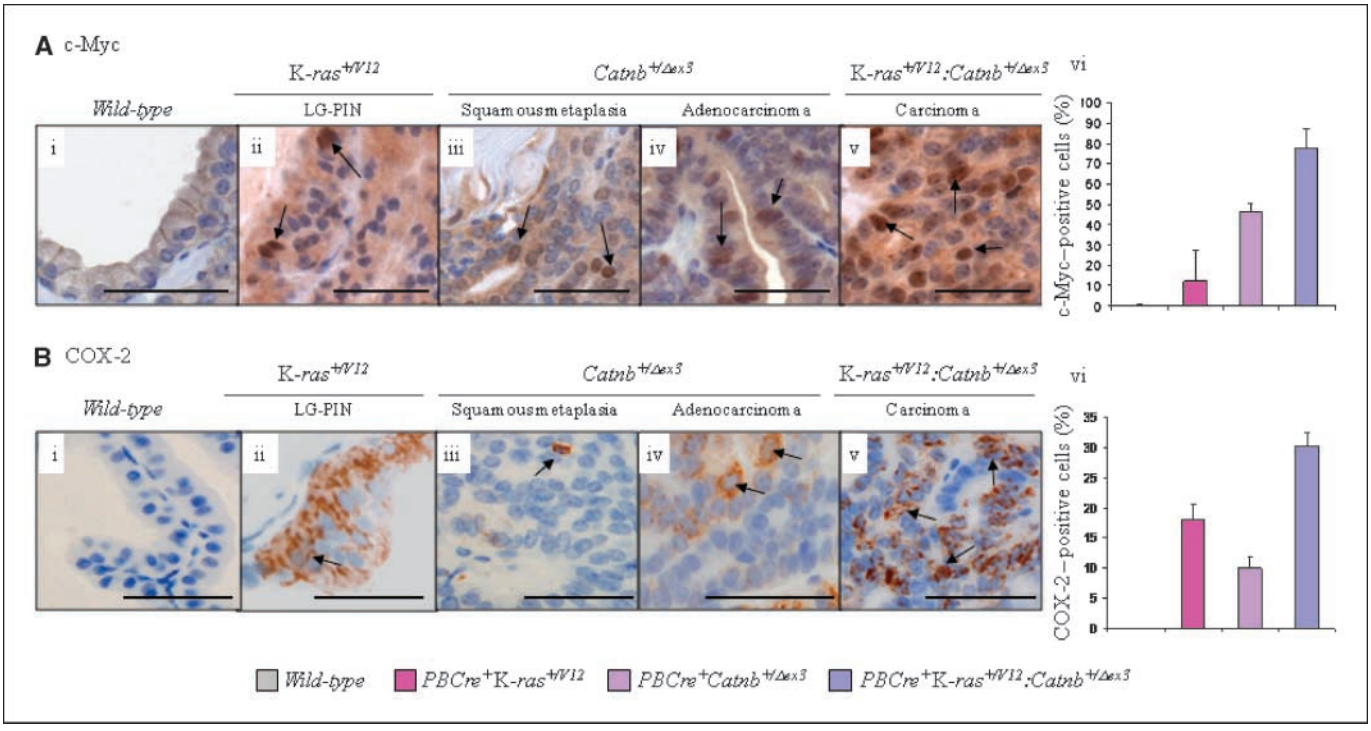

Figure 5. Activating *β-catenin* and *K-ras* mutations synergize via the canonical Wnt pathway to drive prostate tumorigenesis. IHC to detect (*A*) c-Myc and (*B*) COX-2 in *wild-type, PBCre*$^+$*K-ras*$^{+/V12}$, *PBCre*$^+$*Catnb*$^{+/\Delta ex3}$, and *PBCre*$^+$*Catnb*$^{+/\Delta ex3}$*;K-ras*$^{+/V12}$ prostate sections at end point. Images were taken at ×40 magnification; *scale bars,* 50 μm. The percentage of c-Myc (*A, vi*) and COX-2–positive (*B, vi*) prostate epithelial cells were scored for each genotype (n = 3), revealing that *PBCre*$^+$*K-ras*$^{+/V12}$, *PBCre*$^+$*Catnb*$^{+/\Delta ex3}$, and *PBCre*$^+$*Catnb*$^{+/\Delta ex3}$*:K-ras*$^{+/V12}$ prostate tumors showed a significant difference in c-Myc and COX-2 expression compared with *wild-type* mice (P = 0.0404) and to each other (P = 0.0404). *Columns,* mean; *bars,* SD; statistical analysis was carried out using a nonparametric Mann-Whitney test (95% confidence interval).

Counting AR-positive cells revealed that nuclear AR is not highly expressed in *wild-type* prostate at 500 days (5.3%). Transgenic mice displayed a significant elevation in AR expression with tumor progression; K-*ras* mutant LG-PIN (35.8%), *β-catenin* mutant adenocarcinoma (52.6%), and double mutant invasive carcinoma (63.9%; Fig. 4*D*). This coincides with human prostate cancer studies that have observed a similar elevation in AR expression, thus providing the basis for antiandrogen hormone therapy (38). The fact that *PBCre*$^{+}$*Catnb*$^{+/\Delta ex3}$*:K-ras*$^{+/V12}$ mice display the highest level of AR expression may reflect cooperativity between these two oncogenes, possibly owing to MAPK and Wnt signaling mediated AR regulation (16, 39). AR antibody specificity was confirmed by staining sections with additional AR antibodies (Supplementary Fig. S3).

Together, this evidence suggests a synergistic relationship between activating *K-ras*^{V12} and dominant stable *β-catenin* mutations in the mouse prostate. To address this, the expression of c-Myc (Fig. 5*A*) and COX-2 (Fig. 5*B*) were monitored by IHC. The Ras/MAPK and Wnt signaling pathways are known to drive transcription of both c-Myc and COX-2 (6–8). Scoring the percentage of cells positive for nuclear c-Myc expression revealed that *PBCre*$^{+}$ *K-ras*$^{+/V12}$, *PBCre*$^{+}$*Catnb*$^{+/\Delta ex3}$, and *PBCre*$^{+}$*Catnb*$^{+/\Delta ex3}$*:K-ras*$^{+/V12}$ lesions show a progressive increase in nuclear c-Myc (12.03%, 46.22%, and 78.01%, respectively), when compared with wild-type prostate epithelium (0.28%; Fig. 5*Avi*). COX-2 expression at the cell surface of prostate epithelial cells was shown to increase in K-ras and β-catenin mutants (17.81% and 9.83%, respectively) compared with wild-type prostate (0.02%; Fig. 5*Bvi*). These data indicate that activated K-ras in prostate epithelial cells may drive more COX-2 expression than activated β-catenin. Double mutants displayed a further increase in COX-2 expression (30.14%), establishing the synergistic relationship between K-ras and β-catenin oncogenic mutations. Together, this evidence presents a direct mechanism for accelerated prostate tumor progression in double mutants.

Discussion

Here, we show that K-*ras*$^{+/V12}$ alone plays a role in the onset and progression of prostate cancer using a conditional transgenic approach. Activation of K-ras resulted in development of AH and LG-PIN at 100 and 200 to 500 days, respectively, although longevity was not decreased. Consistent with this model, mice expressing *H-Ras*^{V12} driven by the minimal *PB* promoter also developed LG-PIN by 3 months, albeit in conjunction with intestinal metaplasia (17). Given that the *PBCre*$^{+}$K-*ras*$^{+/V12}$ model did not exhibit intestinal metaplasia, it is possible that the *Ras* isoform, genetic background, and the level of cellular stress may play a role in determining the observed phenotype (40). The fact that *PBCre*$^{+}$ K-*ras*$^{+/V12}$ mice showed recombination of the targeted K-*ras*^{V12} allele at 500 days, whereas Scherl and colleagues (17) reported the *H-Ras*^{V12} transgene was not detected in *PB-H-ras*^{V12} mice ≥12 months, suggests that the method of driving transgene expression may also contribute to the phenotypic differences observed.

Consistent with previous work, dominant stabilization of β-catenin predisposed to PIN-like keratinized squamous metaplasia and prostate adenocarcinoma, as well as keratinized squamous metaplasia of the preputial, bulbourethral, and urethral glands (25, 26). *PBCre*$^{+}$*Catnb*$^{+/lox(ex3)}$ mice also displayed reduced survival, which was further reduced in *PBCre*$^{+}$*Catnb*$^{+/\Delta ex3}$*:K-ras*$^{+/V12}$ transgenic mice (Fig. 3*A*). Double mutants showed a synergistic relationship between the activation of K-ras and Wnt signaling pathways, accelerating tumor progression to invasive carcinoma (Fig. 3*B*). The PIN-like keratinized squamous metaplasia observed in the *PBCre*$^{+}$*Catnb*$^{+/lox(ex3)}$ mice was not seen in the K-*ras* mutants, suggesting that this phenotype is specifically generated by aberrant Wnt signaling in the prostate, or that tumor progression beyond the 500 day end-point might be required. Squamous metaplasia was also absent from the double mutant at time of death (average, 189 days); however, we cannot rule out that squamous metaplasia may have occurred in these mice during earlier stages of tumor progression.

Previous work has shown that both Ras and Wnt signaling are able to regulate AR (16, 39). Here, we show an *in vivo* cooperation between K-ras and Wnt leading to synergistic up-regulation of AR in mouse prostate carcinoma in *PBCre*$^{+}$*Catnb*$^{+/\Delta ex3}$*:K-ras*$^{+/V12}$ mice. A 2- to 5-fold increase in AR mRNA is both necessary and sufficient for hormone-refractory progression in animal models, and subsequently, cells can become supersensitive to androgens rather than being independent of them (41). This evidence suggests that the observed increase in cells expressing AR in the *PBCre*$^{+}$-*Catnb*$^{+/\Delta ex3}$ and *PBCre*$^{+}$*Catnb*$^{+/\Delta ex3}$*;K-ras*$^{+/V12}$ prostate tumors may be sufficient to promote androgen-independent prostate growth, correlating to human disease progression. Consistent with this notion, castration studies revealed that *PBCre*$^{+}$*Apc*$^{fl/fl}$ prostate tumors are androgen independent (27).

Given that tumor microenvironments can cause genetic instability and therefore gene mutations, we cannot rule out the possibility that the lesions in our prostate models do not harbor an activating mutation in AR. Indeed, it will be interesting to perform mutational analysis of AR in these lesions to determine whether activated Ras/Wnt signaling in the prostate can generate an environment capable of inducing mutations in AR.

Progressive loss of p63 expression in parallel with tumor progression might reflect elevated MAPK signaling, which has been postulated to regulate p63 expression through Src (42). Kurita and colleagues (42) grafted the UGS from *p63* null mice (which are basal cell deficient) into adult nude males, revealing that prostate development can occur in the absence of basal cells. In this model, luminal cells displayed elevated Ras signaling after increased expression of c-Src in an androgen-dependent manner. Additionally, ΔNp63 has been shown to block β-catenin phosphorylation and nuclear accumulation in squamous cell carcinoma cell lines, suggesting that down-regulation of the ΔNp63 isoform may play a role in further enhancing Wnt signaling (43). Interestingly, p63 expression is suppressed by Notch1 activation in human and mouse keratinocytes (44). This suggests that aberrant Notch signaling may also play a role in promoting prostate tumorigenesis in *PBCre*$^{+}$K-*ras*$^{+/V12}$, *PBCre*$^{+}$*Catnb*$^{+/\Delta ex3}$, and *PBCre*$^{+}$*Catnb*$^{+/\Delta ex3}$*;* K-*ras*$^{+/V12}$ mice. Our data shows that both the Wnt and MAPK signaling transduction cascades effect upon the p63 expressing population. The direct relevance of this to tumor progression remains unclear but is speculated to reflect both the activation of prostate stem cells and the development of androgen-independent prostate growth.

Importantly, the Wnt pathway was not deregulated in *PBCre*$^{+}$*K-ras*$^{+/V12}$ lesions, suggesting that the augmented tumor multiplicity and malignant behavior in compound transgenic mutants is not related to activated K-ras–mediated induction of the Wnt/β-catenin pathway, as shown previously in intestinal studies (2). Expression of activated K-ras (pVillin-*K-ras*^{V12G}) was shown to up-regulate β-catenin nuclear translocation in intestinal tumors, which was further increased in combination with an *Apc* deficiency (*Apc*$^{+/1638N}$; ref. 2). The observation that activated K-ras did not

induce Wnt signaling in our *PBCre*$^{+}$*K-ras*$^{+/V12}$ prostate cancer model suggests that this is probably a tissue specific event.

The synergistic relationship between activated K-ras and dominant stabilization of β-catenin in prostate epithelium was further shown by IHC to detect c-Myc and COX-2. c-Myc is a regulator of cell growth and mutations in this gene are among the most common genetic lesions found in a wide variety of human cancers (45). Recently, conditional deletion of c-Myc from the murine intestine was shown to rescue all the phenotypes of induced *AhCre*$^{+}$*Apc*$^{fl/fl}$ mice (46), demonstrating that c-Myc is required for canonical Wnt-induced tumorigenesis in the intestine. Furthermore, c-Myc expression has also been shown to confer androgen independence in human prostate cancer cells *in vitro* (45). We observe high c-Myc expression in the lesions of the double mutant mice, suggesting these tumors may also be androgen independent. Our data are consistent with previous MPR models, in which activating vHa-*Ras* and *c-Myc* mutations show accelerated tumor progression, demonstrating the cooperativity of these oncogenes in prostate carcinogenesis (19).

To conclude, the *PBCre*$^{+}$*Catnb*$^{+/lox(ex3)}$*:K-ras*$^{+/V12}$ model further establishes the link between aberrant Ras and Wnt signaling in the multistep nature of prostate tumorigenesis and progression, suggesting that a similar interaction may occur in human prostate cancer tumorigenesis. Ultimately, the cooperative up-regulation of AR, c-Myc, and COX-2 via the Ras and Wnt pathways may present a series of novel targets for chemotherapeutic intervention.

Disclosure of Potential Conflicts of Interest

No potential conflicts of interest were disclosed.

Acknowledgments

Received 7/31/2008; revised 10/14/2008; accepted 10/30/2008.

Grant support: Tenovus.

The costs of publication of this article were defrayed in part by the payment of page charges. This article must therefore be hereby marked *advertisement* in accordance with 18 U.S.C. Section 1734 solely to indicate this fact.

We thank Mark Bishop, Lucie Pietzca, Luke Piggott, and Derek Scarborough at Cardiff University for their technical assistance and Brindi Niranjan and Gail Risbrider for the gift of AR antibody.

References

1. Hanahan D, Weinberg R. The hallmarks of cancer. Cell 2000;100:57–70.
2. Janssen K, Alberici P, Fsihi H, et al. APC and oncogenic KRAS are synergistic in enhancing Wnt signaling in intestinal tumor formation and progression. Gastroenterology 2006;131:1096–109.
3. Sansom O, Menial V, Wilkins J, et al. Loss of APC allows phenotypic manifestation of the transforming properties of an endogenous K-ras oncogene *in vivo*. Proc Natl Acad Sci U S A. 2006;103:14122–7.
4. Jang J, Boxer R, Chodosh L. Isoform-specific ras activation and oncogene dependence during MYC- and Wnt-induced mammary tumorigenesis. Mol Cell Biol 2006;26:8106–21.
5. Harada N, Oshima H, Katoh M, Tamai Y, Oshima M, Taketo M. Hepatocarcinogenesis in mice with β-catenin and Ha-ras gene mutations. Cancer Res 2004;64:48–54.
6. Araki Y, Okamura S, Hussain S, et al. Regulation of cyclooxygenase-2 expression by the Wnt and Ras pathways. Cancer Res 2003;63:728–34.
7. He T, Sparks A, Rago C, et al. Identification of c-MYC as a target of the APC pathway. Science 1998;281: 1509–12.
8. Kerkhoff E, Houben R, Löffler S, Troppmair J, Lee J, Rapp U. Regulation of c-myc expression by Ras/Raf signalling. Oncogene 1998;16:211–6.
9. Kranenburg O. The KRAS oncogene: past, present, and future. Biochim Biophys Acta 2005;1756:81–2.
10. Smit V, Boot A, Smits A, Fleuren G, Cornelisse C, Bos J. KRAS codon 12 mutations occur very frequently in pancreatic adenocarcniomas. Nucleic Acids Res 1988;16: 17773–82.
11. Jackson EL, Willis N, Mercer K, et al. Analysis of lung tumor initiation and progression using conditional expression of oncogenic K-ras. Genes Dev 2001;15: 3243–8.
12. Shiraishi T, Muneyuki T, Fukutome K, et al. Mutations of ras genes are relatively frequent in Japanese prostate cancers: pointing to genetic differences between populations. Anticancer Res 1998;18: 2789–92.
13. Uzgare A, Kaplan P, Greenberg N. Differential expression and/or activation of P38MAPK, ERK1/2, and JNK during the initiation and progression of prostate cancer. Prostate 2003;55:128–39.
14. Le-Page C, Koumakpayi I, Alam-Fahmy M, Mes-Masson A, Saad F. Expression and localisation of Akt-1, Akt-2 and Akt-3 correlate with clinical outcome of prostate cancer patients. Br J Cancer 2006;94:1906–12.
15. Weber MJ, Gioeli D. Ras signaling in prostate cancer progression. J Cell Biochem 2004;91:13–25.
16. Carey A, Pramanik R, Nicholson L, et al. Ras-MEK-ERK signaling cascade regulates androgen receptor element-inducible gene transcription and DNA synthesis in prostate cancer cells. Int J Cancer 2007;121:520–7.
17. Scherl A, Li JF, Cardiff RD, Schreiber-Agus N. Prostatic intraepithelial neoplasia and intestinal metaplasia in prostates of probasin-RAS transgenic mice. Prostate 2004;59:448–59.
18. Barrios R, Lebovitz RM, Wiseman AL, et al. RasT24 driven by a probasin promoter induces prostatic hyperplasia in transgenic mice. Transgenics 1996;2:23–8.
19. Thompson T, Southgate J, Kitchener G, Land H. Multistage carcinogenesis induced by ras and myc oncogenes in a reconstituted organ. Cell Commun Signal 1989;56:917–30.
20. Thompson T, Park S, Timme T, et al. Loss of p53 function leads to metastasis in ras+myc-initiated mouse prostate cancer. Oncogene 1995;10:869–79.
21. Morin P, Sparks A, Korinek V, et al. Activation of β-catenin-Tcf signaling in colon cancer by mutations in β-catenin or APC. Science 1997;275:1787–90.
22. Willert K, Nusse R. β-Catenin: a key mediator of Wnt signaling. Curr Opin Genet Dev 1998;8:95–102.
23. Yang X, Chen M, Terry S, et al. Complex regulation of human androgen receptor expression by Wnt signaling in prostate cancer cells. Oncogene 2006;25:3436–44.
24. Chesire D, Ewing C, Gage W, Isaacs W. *In vitro* evidence for complex modes of nuclear β-catenin signaling during prostate growth and tumorigenesis. Oncogene 2002;21:2679–94.
25. Gounari F, Signoretti S, Bronson R, et al. Stabilization of β-catenin induces lesions reminiscent of prostatic intraepithelial neoplasia, but terminal squamous transdifferentiation of other secretory epithelia. Oncogene 2002;21:4099–107.
26. Bierie B, Nozawa M, Renou J, et al. Activation of b-catenin in prostate epithelium induces hyperplasias and squamous transdifferentiation. Oncogene 2003;22: 3875–87.
27. Bruxvoort KJ, Charbonneau HM, Giambernardi TA, et al. Inactivation of Apc in the mouse prostate causes prostate carcinoma. Cancer Res 2007;67:2490–6.
28. Guerra C, Mijimolle N, Dhawahir A, et al. Tumor induction by an endogenous K-ras oncogene is highly dependent on cellular context. Cancer Cell 2003;4: 111–20.
29. Harada N, Tamai Y, Ishikawa T, et al. Intestinal polyposis in mice with a dominant stable mutation of the β-catenin gene. EMBO J 1999;18:5931–42.
30. Wu X, Wu J, Huang J, et al. Generation of a prostate epithelial cell-specific Cre transgenic mouse model for tissue-specific gene ablation. Mech Dev 2001;101:61–9.
31. Ireland H, Kemp R, Houghton C, et al. Inducible Cre-mediated control of gene expression in the murine gastrointestinal tract: effect of loss of β-catenin. Gastroenterology 2004;126:1236–46.
32. Shappell SB, Thomas GV, Roberts RL, et al. Prostate pathology of genetically engineered mice: definitions and classification. The consensus report from the Bar Harbor meeting of the Mouse Models of Human Cancer Consortium Prostate Pathology Committee. Cancer Res 2004;64:2270–305.
33. Pearson H, McCarthy A, Collins C, Ashworth A, Clarke A. Lkb1 deficiency causes prostate neoplasia in the mouse. Cancer Res 2008;68:1–10.
34. Sansom OJ, Reed KR, Hayes AJ, et al. Loss of Apc *in vivo* immediately perturbs Wnt signaling, differentiation, and migration. Genes Dev 2004;18:1385–90.
35. Signoretti S, Waltregny D, Dilks J, et al. p63 is a prostate basal cell marker and is required for prostate development. Am J Pathol 2000;157:1769–75.
36. Urist MJ, Di Como CJ, Lu M-L, et al. Loss of p63 Expression is associated with tumor progression in bladder cancer. Am J Pathol 2002;161:1199–206.
37. Matheny K, Barbieri C, Sniezek J, Arteaga C, Pietenpol J. Inhibition of epidermal growth factor receptor signaling decreases p63 expression in head and neck squamous carcinoma cells. Laryngoscope 2003;113:936–9.
38. Chang C, Heinlein C. Androgen receptor in prostate cancer. Endocr Rev 2004;25:276–308.
39. Truica C, Byers S, Gelmann E. β-catenin affects androgen receptor transcriptional activity and ligand specificity. Cancer Res 2000;60:4709–13.
40. Schubbert S, Shannon K, Bollag G. Hyperactive Ras in developmental disorders and cancer. Nat Rev Cancer 2007;7:295–308.
41. Isaacs J, Isaacs W. Androgen receptor outwits prostate cancer drugs. Nat Med 2004;10:26–7.
42. Kurita T, Medina R, Mills A, Cunha G. Role of p63 and basal cells in the prostate. Development 2004;131: 4955–64.
43. Reis-Filho J, Simpson P, Fulford L, Martins A, Schmitt F. P63-driven nuclear accumulation of β-catenin is not a frequent event in human neoplasms. Pathol Res Pract 2003;199:785–93.
44. Nguyen B, Lefort K, Mandinova A, Antonini D, Devgon V. Cross-regulation between Notch and p63 in keratinocyte commitment to differentiation. Genes Dev 2006;20:1028–42.
45. Bernard D, Pourtier-Manzanedo A, Gil J, Beach D. Myc confers androgen-independent prostate cancer cell growth. J Clin Invest 2003;112:1724–31.
46. Sansom OJ, Meniel VS, Muncan V, et al. Myc deletion rescues Apc deficiency in the small intestine. Nature 2007;446:676–9.